Macroscopic quantum tunnelling of a ^{7}Li condensate in a cylindrical trap

2001 J. Phys. A: Math. Gen. 34 2643

(http://iopscience.iop.org/0305-4470/34/12/311)

INSTITUTE OF PHYSICS PUBLISHING JOURNAL OF PHYSICS A: MATHEMATICAL AND GENERAL

J. Phys. A: Math. Gen. **34** (2001) 2643–2655 www.iop.org/Journals/ja PII: S0305-4470(01)19649-6

Macroscopic quantum tunnelling of a ^{7}Li condensate in a cylindrical trap

Yukinori Yasui, Takayuki Takaai and Takayoshi Ootsuka

Department of Physics, Osaka City University, Sumiyoshiku, Osaka, Japan

E-mail: yasui@sci.osaka-cu.ac.jp, takaai@sci.osaka-cu.ac.jp and ootsuka@sci.osaka-cu.ac.jp

Received 24 November 2000, in final form 9 February 2001

Abstract

We investigate the macroscopic quantum tunnelling of a ^{7}Li condensate. Within the effective Lagrangian framework provided by the time-dependent variational principle approach, we find bounce solutions and explicitly calculate the decay rate of the condensate trapped in a cylindrically symmetric potential. In particular, in the case where the number of condensed bosons is slightly below a certain critical number, we present a detailed analysis of the bounce solutions and discuss the approximations employed in our calculations. The effects of finite temperatures and the shape of the trapping potential are evaluated.

PACS numbers: 0375F, 0365

(Some figures in this article are in colour only in the electronic version; see www.iop.org)

1. Introduction

Macroscopic quantum tunnelling is an interesting subject in many areas of physical sciences including low-temperature physics, atomic physics and nuclear physics. Recent realization of the Bose–Einstein condensate of trapped alkali atoms may provide a good testing ground for the investigation of this problem [1].

In this paper we will discuss the macroscopic quantum tunnelling of a ^{7}Li condensate. The dynamics of the condensate is successfully described by the Gross–Pitaevskii (GP) equation [2, 3]. The s-wave scattering length a entering the GP equation can be positive or negative, its sign and magnitude depending crucially on the details of the atom–atom interaction. In the case of ^{7}Li, the interaction is attractive and the scattering length is known to be $a = -1.45 \pm 0.04$ nm [4, 5]. The attractive interaction causes the condensate to collapse upon itself. When the trapping potential is included, however, the destabilizing influence of the interaction is balanced by the zero-point kinetic energy, thereby allowing a metastable condensate to form [6–8]. Pérez-García *et al* [6] have investigated the GP equation by using a time-dependent variational technique [9, 10]. Their results reproduce quite accurately the low-energy excitation spectrum of the condensate obtained by numerical simulations of the GP equation. We will apply this variational technique to the macroscopic tunnelling of the metastable condensate of ^{7}Li. When the trapping is spherically symmetric, Ueda and Leggett [11] have evaluated the tunnelling decay rate at zero temperature (see also [7, 12]). In this paper we develop their analysis and explicitly write down the decay rate in the case of a cylindrically symmetric trapping potential and further finite temperatures.

In section 2, according to [6], we derive an effective Lagrangian describing the Bose–Einstein condensate of ^{7}Li, and summarize the data of the ground-state energy that we shall need in the calculations of tunnelling. In section 3, we present a detailed analysis of bounce solutions. Using the effective Lagrangian and with the help of numerical simulations, we find the bounce solutions. We next consider the special situation where the number of condensed bosons is slightly below a certain critical number. Then the effective Lagrangian reduces to a simple one-dimensional Lagrangian by appropriate approximations. We present an analytic solution for the bounce within this situation, and explicitly calculate the decay rate of the metastable condensate. We also evaluate the decay rate at finite temperatures and predict a critical temperature, where the rate crosses over from quantum tunnelling to thermal hopping. Section 4 is devoted to the summary of our findings.

2. Model

We consider gases of ^{7}Li atoms trapped in a cylindrically symmetric harmonic potential

$$V(x, y, z) = \tfrac{1}{2} m\nu^2 (x^2 + y^2 + \lambda^2 z^2) \tag{1}$$

where λ represents the asymmetry parameter of the trapping potential. The dynamics of the condensate is described by the GP Lagrangian

$$\mathcal{L} = \frac{\mathrm{i}\hbar}{2}\left(\psi \frac{\partial \psi^*}{\partial t} - \frac{\partial \psi}{\partial t}\psi^*\right) - \frac{\hbar^2}{2m}|\nabla \psi|^2 - V|\psi|^2 - \frac{2\pi\hbar^2 a}{m}|\psi|^4. \tag{2}$$

In order to obtain the evolution of the condensate wavefunction, we assume the Gaussian form for the wavefunction according to [6]:

$$\psi(x, y, z, t) = A(t) \prod_{a=x,y,z} \exp\left[-\frac{(x_a - \eta_a(t))^2}{2W_a(t)^2} + \mathrm{i}x_a\alpha_a(t) + \mathrm{i}x_a^2\beta_a(t)\right]. \tag{3}$$

This trial function includes the time-dependent variational parameters, $\boldsymbol{\eta} = (\eta_x, \eta_y, \eta_z)$ (centre coordinate), $\boldsymbol{W} = (W_x, W_y, W_z)$ (width) and the phase parameters $\boldsymbol{\alpha} = (\alpha_x, \alpha_y, \alpha_z)$, $\boldsymbol{\beta} = (\beta_x, \beta_y, \beta_z)$, which correspond to the 'momenta' canonically conjugate to $\boldsymbol{\eta}$ and $\boldsymbol{W}$. The wavefunction ψ is normalized by the number of condensed bosons $N = \int |\psi|^2 \,\mathrm{d}^3x$, so that the parameter A (amplitude) is given by

$$A = \frac{1}{\pi^{3/4}}\sqrt{\frac{N}{W_x W_y W_z}}. \tag{4}$$

Substituting (3) into (2) and further integrating the GP Lagrangian over space coordinates, one obtains an effective quantum mechanical Lagrangian

$$\mathcal{L}_{\mathrm{eff}} = \sum_{a=x,y,z} (p_a\dot{\eta}_a + K_a\dot{W}_a) - \mathcal{H}_{\mathrm{eff}}(\eta_a, W_a, p_a, K_a) \tag{5}$$

where p_a and K_a are the momenta canonically conjugate to η_a and W_a defined by

$$p_a = \hbar N(\alpha_a + 2\eta_a\beta_a) \tag{6}$$

$$K_a = \hbar N\beta_a W_a. \tag{7}$$

The Hamiltonian $\mathcal{H}_{\text{eff}} = \mathcal{H}_0 + \mathcal{H}_1$ consists of two parts: the first part $\mathcal{H}_0$ simply describes the harmonic oscillation of the centre of the condensate

$$\mathcal{H}_0 = \sum_{a=x,y,z} \frac{1}{2mN} p_a^2 + \frac{Nm\nu^2}{2}(\eta_x^2 + \eta_y^2 + \lambda^2\eta_z^2) \tag{8}$$

and the remaining part $\mathcal{H}_1$ describes the evolution of the widths of the condensate

$$\mathcal{H}_1 = \sum_{a=x,y,z} \frac{1}{mN} K_a^2 + \hat{U}(\boldsymbol{W}) \tag{9}$$

with

$$\hat{U}(\boldsymbol{W}) = \frac{mN\nu^2}{4}(W_x^2 + W_y^2 + \lambda^2 W_z^2) + \frac{\hbar^2 N}{4m}\left(\frac{1}{W_x^2} + \frac{1}{W_y^2} + \frac{1}{W_z^2}\right) + \frac{a\hbar^2 N^2}{\sqrt{2\pi}m}\frac{1}{W_x W_y W_z}. \tag{10}$$

It is convenient to introduce the scales characterizing the trapping potential: (a) length scale $a_0 = \sqrt{\hbar/m\nu}$, (b) energy scale $e_0 = \hbar\nu/2$, (c) timescale ν^{-1}. By using these units we define dimensionless quantities, $\boldsymbol{\xi} = a_0^{-1}\boldsymbol{\eta}$, $\boldsymbol{X} = a_0^{-1}\boldsymbol{W}$ and $\tau = \nu t$. Then the Lagrangian (5) is rescaled as follows:

$$L_{\text{eff}} = e_0^{-1}\mathcal{L}_{\text{eff}} = L_0 + L_1 \tag{11}$$

where

$$L_0 = N\left(\frac{\mathrm{d}\boldsymbol{\xi}}{\mathrm{d}\tau}\right)^2 - N(\xi_x^2 + \xi_y^2 + \lambda^2\xi_z^2) \tag{12}$$

and

$$L_1 = \frac{N}{2}\left(\frac{\mathrm{d}\boldsymbol{X}}{\mathrm{d}\tau}\right)^2 - NU(\boldsymbol{X}) \tag{13}$$

$$U(\boldsymbol{X}) = \frac{1}{2}(X^2 + Y^2 + \lambda^2 Z^2) + \frac{1}{2}\left(\frac{1}{X^2} + \frac{1}{Y^2} + \frac{1}{Z^2}\right) + \frac{P}{XYZ} \tag{14}$$

with $P = \sqrt{2/\pi}Na/a_0 < 0$. We now focus our attention on the ground-state energy of the condensed Bose system. Under the present analysis, the ground-state energy can be calculated by finding the critical points of U and the eigenvalues of the Hessian matrix

$$F = \begin{pmatrix} \dfrac{\partial^2 U}{\partial X\partial X} & \dfrac{\partial^2 U}{\partial X\partial Y} & \dfrac{\partial^2 U}{\partial X\partial Z} \\ \dfrac{\partial^2 U}{\partial Y\partial X} & \dfrac{\partial^2 U}{\partial Y\partial Y} & \dfrac{\partial^2 U}{\partial Y\partial Z} \\ \dfrac{\partial^2 U}{\partial Z\partial X} & \dfrac{\partial^2 U}{\partial Z\partial Y} & \dfrac{\partial^2 U}{\partial Z\partial Z} \end{pmatrix} \tag{15}$$

evaluated on the critical points.

2.1. *Critical points*

The critical points are given by the solutions to $\partial U/\partial \boldsymbol{X} = 0$. They satisfy the equations

$$X = Y \tag{16}$$

$$\frac{1}{Z^4} + \frac{P}{X^2 Z^3} = \lambda^2 \tag{17}$$

$$\frac{1}{X^4} + \frac{P}{X^4 Z} = 1. \tag{18}$$

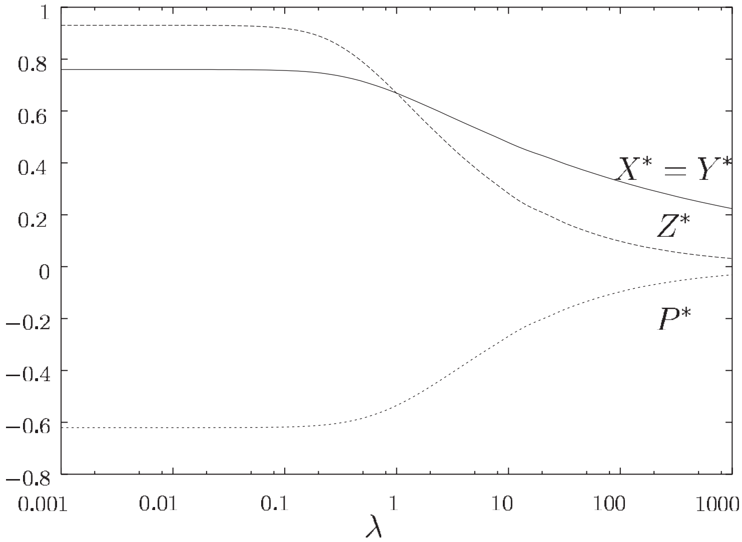

Figure 1. λ-dependence of P^* and $\boldsymbol{X}^* = (X^*, Y^*, Z^*)$.

The solutions are classified by the critical value P^* of the parameter P; when $|P| > |P^*|$, there are no critical points. When $|P| < |P^*|$, there are two critical points, one stable (Morse index = 0) and the other unstable (Morse index = 1) [6]. The critical value P^* also satisfies in addition to the equations (16)–(18)

$$\frac{P}{X^2 Z^3} + \frac{1}{2}\frac{P^2}{X^6 Z^4} = 4\lambda^2 \tag{19}$$

which can be derived from the condition $\epsilon_T = 0$ (see (24)). Thus, P^* and the corresponding coordinate $\boldsymbol{X}^* = (X^*, Y^*, Z^*)$ are uniquely determined as a function of the asymmetry parameter λ. Indeed we have $P^* = -4/5^{5/4}$, $\boldsymbol{X}^* = 5^{-1/4}(1, 1, 1)$ for $\lambda = 1$, and general solutions are provided in figure 1. It should be noticed that for $P \to P^*$ the stable critical point $\boldsymbol{X}_{\rm s}$ and the unstable critical point $\boldsymbol{X}_{\rm u}$ take the following asymptotic forms:

$$\boldsymbol{X}_{\rm s} = \boldsymbol{X}^* + k(1 - P/P^*)^{1/2}\boldsymbol{E} + \mathcal{O}(1 - P/P^*) \tag{20}$$

$$\boldsymbol{X}_{\rm u} = \boldsymbol{X}^* - k(1 - P/P^*)^{1/2}\boldsymbol{E} + \mathcal{O}(1 - P/P^*) \tag{21}$$

where $\boldsymbol{E} = (-P^*_{32}, -P^*_{32}, 1)$ and the coefficient k is given by

$$k = \sqrt{\frac{2}{3}}\left(\frac{P^*_{21}(2P^*_{41} - 1)}{2\lambda^2(1 - P^*_{41}) - P^*_{23}}\right)^{\frac{1}{2}} \tag{22}$$

with $P^*_{ij} = P^*/4(X^*)^i(Z^*)^j$.

2.2. *Eigenvalues of Hessian matrix*

For the eigenvalue problem of the Hessian matrix evaluated on the critical points

$$F e_A = \epsilon_A^2 e_A \qquad (A = T, N, B) \tag{23}$$

we have the following results [6]:

(a) T-direction

$$\epsilon_T^2 = 2\left(\lambda^2 + 1 - P_{23} - \sqrt{8(P_{32})^2 + (1-\lambda^2+P_{23})^2}\right) \quad (24)$$

$$\boldsymbol{e}_T = \frac{1}{\triangle_T}(s_{\shortparallel}, s_{\shortparallel}, P_{32}) \quad (25)$$

$$\text{with} \quad s_{\shortparallel} = \tfrac{1}{4}\left(-\lambda^2 + 1 + P_{23} - \sqrt{8(P_{32})^2 + (1-\lambda^2+P_{23})^2}\right). \quad (26)$$

(b) N-direction

$$\epsilon_N^2 = 2\left(\lambda^2 + 1 - P_{23} + \sqrt{8(P_{32})^2 + (1-\lambda^2+P_{23})^2}\right) \quad (27)$$

$$\boldsymbol{e}_N = \frac{1}{\triangle_N}(s_\perp, s_\perp, P_{32}) \quad (28)$$

$$\text{with} \quad s_\perp = \tfrac{1}{4}\left(-\lambda^2 + 1 + P_{23} + \sqrt{8(P_{32})^2 + (1-\lambda^2+P_{23})^2}\right). \quad (29)$$

(c) B-direction

$$\epsilon_B^2 = 4(1 - 2P_{41}) \quad (30)$$

$$\boldsymbol{e}_B = \frac{1}{\sqrt{2}}(1, -1, 0). \quad (31)$$

Here we used the notation

$$P_{ij} = \frac{P}{4X^i Z^j} \qquad (|P| \leqslant |P^*|) \quad (32)$$

and

$$\triangle_{T,N}^2 = 2(P_{32})^2 + \tfrac{1}{4}\left[(P_{23} + 1 - \lambda^2)^2 \mp (P_{23} + 1 - \lambda^2)\sqrt{8(P_{32})^2 + (1-\lambda^2+P_{23})^2}\right] \quad (33)$$

by the normalization $\boldsymbol{e}_A \cdot \boldsymbol{e}_B = \delta_{AB}$. It should be noticed that the eigenvalue ϵ_T^2 is positive (negative) for the stable (unstable) critical point and the other eigenvalues are all positive.

2.3. Ground state

We restrict the condensate wavefunction ψ to the trial function represented by the variational parameters,

$$\mathcal{B} = \{(\boldsymbol{X}, \boldsymbol{\xi}, \boldsymbol{\alpha}, \boldsymbol{\beta}) | \boldsymbol{X} = \boldsymbol{X}_\mathrm{s} + \sum_{A=T,N,B} y_A \boldsymbol{e}_A \text{ and } |y_A| \ll 1\} \quad (34)$$

where $\boldsymbol{e}_A$ stands for the eigenvector of the Hessian matrix. Then, the GP energy functional corresponding to (2),

$$H[\psi] = \int \mathrm{d}^3x \left(\frac{\hbar^2}{2m}|\nabla\psi|^2 + V|\psi|^2 + \frac{2\pi\hbar^2 a}{m}|\psi|^4\right) \quad (35)$$

takes the form

$$H[\psi] = e_0 N U(\boldsymbol{X}_\mathrm{s}) + e_0 N \left(\left(\frac{\mathrm{d}\boldsymbol{\xi}}{\mathrm{d}\tau}\right)^2 + \xi_x^2 + \xi_y^2 + \lambda^2 \xi_z^2\right)$$
$$+ \frac{e_0 N}{2} \sum_{A=T,N,B} \left(\left(\frac{\mathrm{d}y_A}{\mathrm{d}\tau}\right)^2 + \epsilon_A^2(\boldsymbol{X}_\mathrm{s}) y_A^2\right) + \mathcal{O}(y_A^3) \quad (36)$$

where the first term is the potential energy evaluated on the stable critical point $\boldsymbol{X}_\mathrm{s}$, and the second and third terms represent the harmonic oscillations of the condensate. This result implies the following approximate ground-state energy:

$$e_0^{-1} E_g \simeq N U(\boldsymbol{X}_\mathrm{s}) + (2 + \lambda) + \sum_{A=T,N,B} \epsilon_A(\boldsymbol{X}_\mathrm{s}). \quad (37)$$

3. Macroscopic quantum tunnelling

In this section we argue the macroscopic quantum tunnelling of the Bose condensate using the Lagrangian (13). The stable critical point $\boldsymbol{X}_s$ of the potential $U(\boldsymbol{X})$ represents a metastable condensate since the parameter P in $U(\boldsymbol{X})$ is negative, and so the ground-state energy will have an (exponentially small) imaginary part in addition to (37) if we take account of the tunnelling. The decay rate of the metastable condensate is determined from [13]

$$\Gamma = \frac{2}{\hbar}\mathrm{Im}\, E_g. \tag{38}$$

We will calculate the decay rate by using the WKB approximation. Since the Lagrangian (13) includes a macroscopic quantity N representing the number of condensed bosons, we must be careful in the choice of a small parameter h controlling the validity of the WKB approximation. The precise value of h is given by (58), and the decay rate is of the form

$$\Gamma \simeq A \exp\left(-\frac{S_{cl}}{h}\right) \tag{39}$$

where S_{cl} is the Euclidean action evaluated at the bounce solution and A the square root of the determinant of the second variation around the bounce solution, with the zero mode removed.

3.1. Zero temperature

In order to evaluate the decay rate (39), we use the effective Lagrangian (11). The first term L_0 simply describes a harmonic oscillation and so it does not contribute to the decay rate. After a Wick rotation to an Euclidean time, the relevant action is given by

$$\frac{S_E}{\hbar} = \frac{N}{2}\int_{-\infty}^{\infty} d\tau \left(\frac{1}{2}\left(\frac{d\boldsymbol{X}}{d\tau}\right)^2 + U(\boldsymbol{X})\right) \tag{40}$$

where $U(\boldsymbol{X})$ is the potential given by (14). The bounce solution is the classical solution to the equations of motion

$$\frac{d^2}{d\tau^2}X - X + \frac{1}{X^3} + P\frac{1}{X^2YZ} = 0 \tag{41}$$

$$\frac{d^2}{d\tau^2}Y - Y + \frac{1}{Y^3} + P\frac{1}{XY^2Z} = 0 \tag{42}$$

$$\frac{d^2}{d\tau^2}Z - \lambda^2 Z + \frac{1}{Z^3} + P\frac{1}{XYZ^2} = 0 \tag{43}$$

subject to the boundary condition

$$\lim_{\tau\to\pm\infty} \boldsymbol{X}(\tau) = \boldsymbol{X}_s \text{ (stable critical point)}. \tag{44}$$

In figure 2, we show the behaviour of bounce solutions obtained using numerical simulations.

Let us investigate analytically the system (40) by choosing a parameter P near the critical value P^*. Then the bounce solution $\boldsymbol{X}_b(\tau)$ is restricted in the neighbourhood of the stable critical point $\boldsymbol{X}_s$. Indeed, the equations (20) and (21) give the estimation

$$|\boldsymbol{X}_b(\tau) - \boldsymbol{X}_s| \sim |\boldsymbol{X}_s - \boldsymbol{X}_u| \sim \mathcal{O}((1 - P/P^*)^{1/2}). \tag{45}$$

In the following text we will assume

$$\delta = 1 - P/P^* \sim 10^{-3} \qquad |P| < |P^*|. \tag{46}$$

This parameter region is particularly interesting; as seen later on the value $S_E/\hbar$ is of the order of unity, in this region, though the prefactor N in the action is very large (the number of atoms

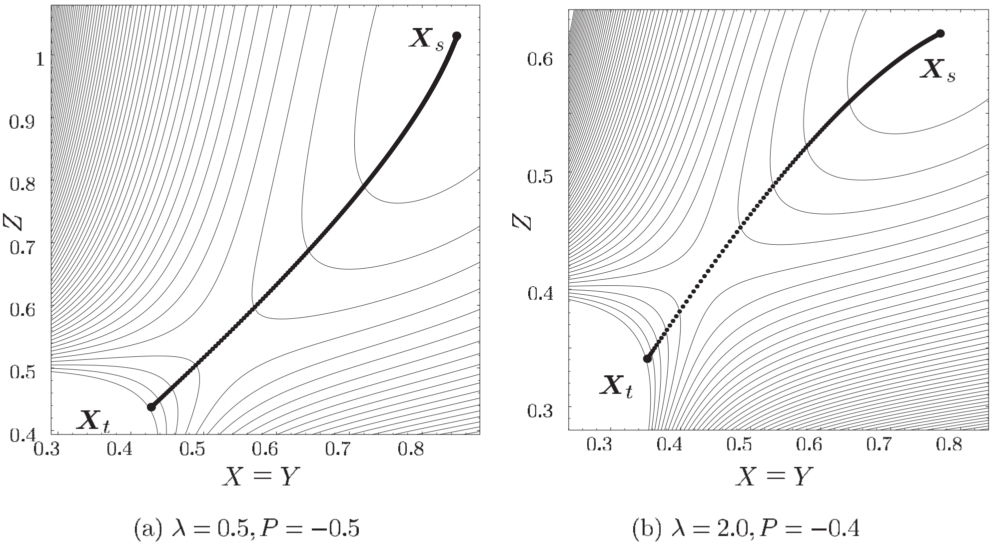

Figure 2. Behaviour of the bounce solution. The bold-faced curve connecting the two points, $\boldsymbol{X}_\mathrm{s}$ (stable critical point) and $\boldsymbol{X}_\mathrm{t}$ (turning point) corresponds to the bounce solution. The solid curves represent the contours of the potential $U(\boldsymbol{X})$. Parameter values: $\delta = 1 - P/P^* = 0.144$ for (*a*) and $\delta = 0.135$ for (*b*).

used in the experiment at Rice University is of the order of 10^3 [14, 15]). Thus we can expect to observe the macroscopic quantum tunnelling by experiments.

We now introduce a new coordinate $\boldsymbol{x} = (x_T, x_N, x_B)$ around $\boldsymbol{X}_\mathrm{s}$

$$\boldsymbol{X} = \boldsymbol{X}_\mathrm{s} + \sum_{A=T,N,B} x_A \boldsymbol{e}_A \tag{47}$$

and expand the potential

$$U(\boldsymbol{X}) = U(\boldsymbol{X}_\mathrm{s}) + \frac{1}{2} \sum_{A=T,N,B} \epsilon_A^2 x_A^2 + \sum_{n+m+l=3} c_{nml} x_T^n x_N^m x_B^l + \cdots. \tag{48}$$

It should be noticed that the eigenvalue ϵ_T approaches zero for $\delta \to 0$. Indeed, we can evaluate the behaviour of ϵ_T near P^* using the exact formula (24):

$$\epsilon_T = \alpha\delta^{1/4} + \mathcal{O}(\delta^{3/4}) \tag{49}$$

where

$$\alpha^2 = \frac{4}{\lambda^2 + 1 - P_{23}^*} \sqrt{(-6P_{23}^*)(1 - 2P_{41}^*)(2\lambda^2(1 - P_{41}^*) - P_{23}^*)}. \tag{50}$$

On the other hand, eigenvalues ϵ_N and ϵ_B can be approximated by (27) and (30) evaluated on P^*, and these values become extremely large compared with ϵ_T when the parameter δ approaches zero. This means that the direction of the initial (infinitesimal) velocity of the bounce solution is given by the eigenfunction $\boldsymbol{e}_T$. Thus the trajectory of the bounce solution is mainly described by $x(\tau) = x_T(\tau)$, i.e. the T-component of the coordinate $\boldsymbol{x}(\tau)$, and remaining components $x_N(\tau)$ and $x_B(\tau)$ give higher-order corrections. More precisely, using (48) and (49), we can evaluate the bounce solution as $x_T(\tau) \sim \mathcal{O}(\delta^{1/2})$, $x_N(\tau) \sim \mathcal{O}(\delta)$ and $x_B(\tau) = 0$ by the symmetry of the equations of motion (if we specialize to the spherically symmetric trapping potential,

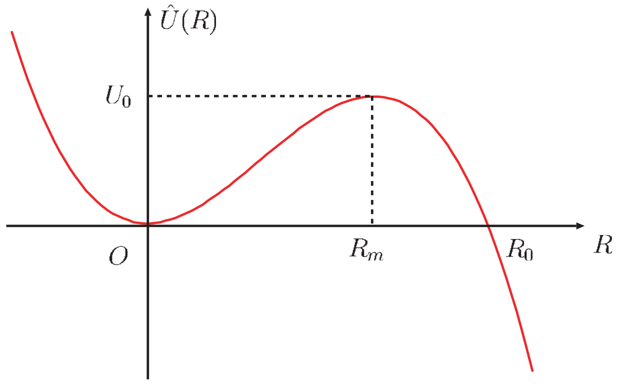

Figure 3. Potential profile for $\delta \to 0$. The potential $\hat{U}(\boldsymbol{W})$ given by (10) is approximated by a one-dimensional potential $\hat{U}(R) = e_0 N((\epsilon_T^2/2)x^2 + (c/3!)x^3)$ with $R = a_0 x$. The potential $\hat{U}(R)$ has a metastable minimum at $R = 0$ and a barrier of height $U_0 = \hat{U}(R_m)$, $R_m = 2a_0\epsilon_T^2/|c|$.

the N-component $x_N(\tau)$ exactly vanishes). We now approximate (40) by one-dimensional quantum mechanical action:

$$\frac{S_E}{\hbar} \simeq \frac{N}{2}\int_{-\infty}^{\infty} \mathrm{d}\tau \left(\frac{1}{2}\left(\frac{\mathrm{d}x}{\mathrm{d}\tau}\right)^2 + \frac{1}{2}\epsilon_T^2 x^2 + \frac{c}{3!}x^3\right). \tag{51}$$

From (25) and (26), the coefficient $c(<0)$ is given by

$$c = \frac{1}{\triangle_T^3}\left\{2s_{\shortparallel}^3\left(\frac{\partial^3 U}{\partial X^3} + 3\frac{\partial^3 U}{\partial X^2 \partial Y}\right) + P_{32}^3\frac{\partial^3 U}{\partial Z^3} + 18 s_{\shortparallel}^2 P_{32}\frac{\partial^3 U}{\partial X \partial Y \partial Z} + 6 s_{\shortparallel} P_{32}^2 \frac{\partial^3 U}{\partial X \partial Z^2}\right\}\Bigg|_{\boldsymbol{X}=\boldsymbol{X}_s} \tag{52}$$

which takes the following asymptotic form:

$$c = -12(P_{24}^* + 4P_{41}^* P_{24}^* - 2\lambda^2 P_{42}^*)(1 + 2(P_{32}^*)^2)^{-3/2} + \mathcal{O}(\delta^{1/2}). \tag{53}$$

It is convenient to introduce new scales characterizing the quantum tunnelling: according to figure 3 we define

$$\text{(a) length scale } R_0 = \frac{3a_0\epsilon_T^2}{|c|} = \frac{3a_0\alpha^2}{|c|}\delta^{1/2}(1 + \mathcal{O}(\delta^{1/2})) \tag{54}$$

$$\text{(b) energy scale } U_0 = \frac{N\hbar\nu\epsilon_T^6}{3c^2} = \frac{N\hbar\nu\alpha^6}{3c^2}\delta^{3/2}(1 + \mathcal{O}(\delta^{1/2})). \tag{55}$$

Then we have a natural timescale

$$T_0 = \frac{R_0}{(2U_0/Nm)^{1/2}} = \frac{\omega_0}{\nu\alpha}\delta^{-1/4}(1 + \mathcal{O}(\delta^{1/2})) \qquad \omega_0 = \sqrt{\frac{27}{2}} \tag{56}$$

representing the 'tunnelling time'.

Now the action (51) is of the form

$$\frac{S_E}{\hbar} = \frac{1}{h}\int_{-\infty}^{\infty} \mathrm{d}s \left(\frac{1}{2}\left(\frac{\mathrm{d}q}{\mathrm{d}s}\right)^2 + \tilde{U}(q)\right) \qquad \tilde{U}(q) = \tfrac{1}{2}\omega_0^2 q^2(1-q) \tag{57}$$

where we have used rescaled quantities, $q = (a_0/R_0)x$ and $s = (1/\nu T_0)\tau$. The prefactor (effective Planck's constant)

$$h = \frac{\hbar}{U_0 T_0} = \frac{2\omega_0 c^2}{9N\alpha^5}\delta^{-5/4}(1 + \mathcal{O}(\delta^{1/2})) \tag{58}$$

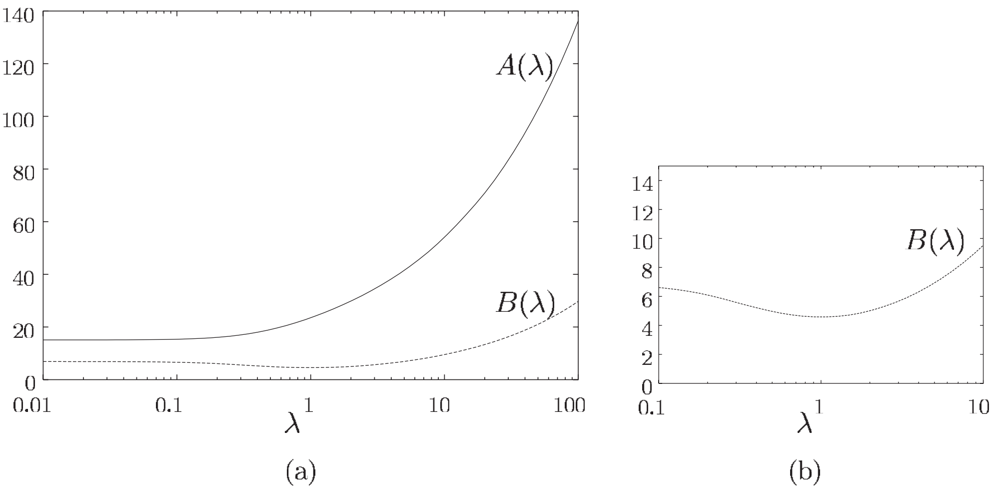

Figure 4. (*a*) λ-dependence of the functions A and B, and (*b*) the detail of $B(\lambda)$ in the region of $\lambda = 1$.

is a dimensionless parameter controlling the validity of the WKB approximation. The equations of motion associated with (57) can be easily integrated, yielding the well known bounce solution

$$q_{\rm b}(s) = \mathrm{sech}^2\left(\frac{\omega_0 s}{2}\right). \tag{59}$$

Using the WKB approximation [13], we obtain the decay rate

$$\Gamma_0 = \left(4\sqrt{\frac{\omega_0^3}{\pi h}}\exp\left(-\frac{S_{\rm cl}}{h}\right)\right)(1+\mathcal{O}(h))T_0^{-1} \tag{60}$$

with the bounce action $S_{\rm cl} = \frac{8}{15}\omega_0$. It follows from (56) and (58) that for $\delta \to 0$ the leading contribution to Γ_0 is given by

$$\frac{\Gamma_0}{\nu} \simeq A\sqrt{N}\delta^{7/8}\exp(-BN\delta^{5/4}). \tag{61}$$

Here, the coefficients A and B are functions of the asymmetry parameter λ:

$$A = 4\sqrt{\frac{9}{2\pi}}\frac{\alpha^{7/2}}{|c|} \qquad B = \frac{12\alpha^5}{5c^2} \tag{62}$$

which can be calculated by (50) and (53). Figure 4 shows the λ-dependence of these coefficients. The spherically symmetric trapping potential ($\lambda = 1$) minimizes the function B and its value is 4.58 in excellent agreement with the result of [11]. The functions A, B remain relatively constant for $\lambda < 1$ but they grow for $\lambda > 1$. For $\delta \to 0$ the tunnelling exponent and the prefactor vanish according to $\delta^{5/4}$ and $\delta^{7/8}$, respectively [11, 12]. We find that this scaling law is universal, independent of the shape of the harmonic trapping potential.

3.2. Finite temperature

In the case of finite temperature β^{-1}, the bounce solution is given by a periodic solution, i.e. the classical solution in the potential $-\tilde{U}(q)$ with energy $-E(0 < E < 1)$. From figure 5 the solution takes the form [16]

$$q_{\rm b}(s) = q_2 - (q_2 - q_1)\mathrm{sn}^2\left(\frac{\omega_0}{2}\sqrt{q_2 - q_0}s; m\right) \tag{63}$$

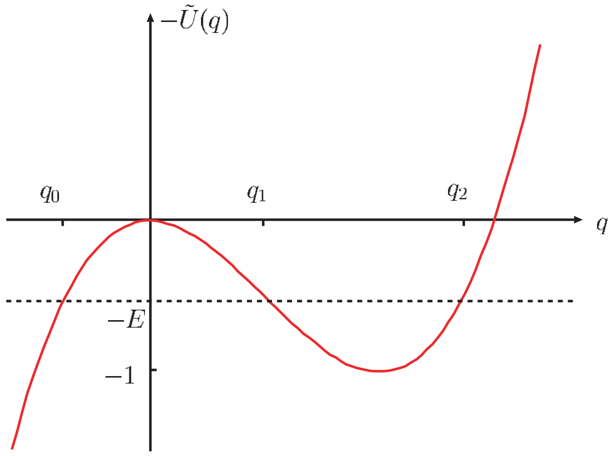

Figure 5. Turning points in the potential $\tilde{U}(q) = \frac{1}{2}\omega_0^2 q^2(1-q)$, $\omega_0 = \sqrt{27/2}$. The 'energy' $E(0 < E < 1)$ is determined as a function of β by requiring that the motion between the turning points q_1 and q_2 is periodic, with period βh.

with the elliptic modulus $m = \sqrt{\frac{q_2-q_1}{q_2-q_0}}$ and the period $h\beta$ is given by the complete elliptic integral of the first kind:

$$h\beta = \frac{4}{\omega_0\sqrt{q_2-q_0}}K(m) \qquad K(m) = \int_0^1 \frac{\mathrm{d}x}{\sqrt{(1-x^2)(1-mx^2)}}. \tag{64}$$

This solution reduces, of course, to the previous solution (59) for $E = 0$. The corresponding bounce action is evaluated as

$$\begin{aligned} S_{\mathrm{cl}} &= \int_0^{h\beta} \mathrm{d}s \left(\frac{1}{2}\left(\frac{\mathrm{d}q_{\mathrm{b}}}{\mathrm{d}s}\right)^2 + \tilde{U}(q_{\mathrm{b}}) \right) \\ &= W + h\beta E \end{aligned} \tag{65}$$

where

$$\begin{aligned} W = \frac{4\omega_0}{15}\sqrt{q_2-q_0}[2(q_0^2+q_1^2+q_2^2-q_0q_1-q_0q_2-q_1q_2)E(m) \\ +(q_1-q_0)(2q_0-q_1-q_2)K(m)]. \end{aligned} \tag{66}$$

($E(m)$ is the complete elliptic integral of the second kind.) The fluctuation modes about the bounce solution include a zero mode $\phi_1(s) = \dot{q}_{\mathrm{b}}(s)$. Then the determinant factor A in (39) is calculated from the Gelfand–Yaglom formula [17, 18]:

$$A(\beta) = \frac{1}{\sqrt{\pi h}}\sqrt{\frac{\dot{\phi}_1(s)}{\dot{\phi}_2(s)}}\sinh(\omega_0 s)\Bigg|_{s=\beta h/2} \qquad \phi_2(s) = \phi_1(s)\int^s \frac{\mathrm{d}s'}{\phi_1(s')^2}. \tag{67}$$

Thus we obtain the finite-temperature decay rate due to quantum tunnelling:

$$\Gamma(\beta) = \left(A(\beta)\exp\left(\frac{-S_{\mathrm{cl}}}{h}\right)\right)(1+\mathcal{O}(h))T_0^{-1} \tag{68}$$

where

$$A(\beta) = \sqrt{\frac{\omega_0^3}{2\pi h}\frac{(q_2-q_0)^{3/4}(q_2-q_1)(1-m^2)}{(a(m)E(m)+b(m)K(m))^{1/2}}}\sinh\left(\frac{\omega_0\beta h}{2}\right) \tag{69}$$

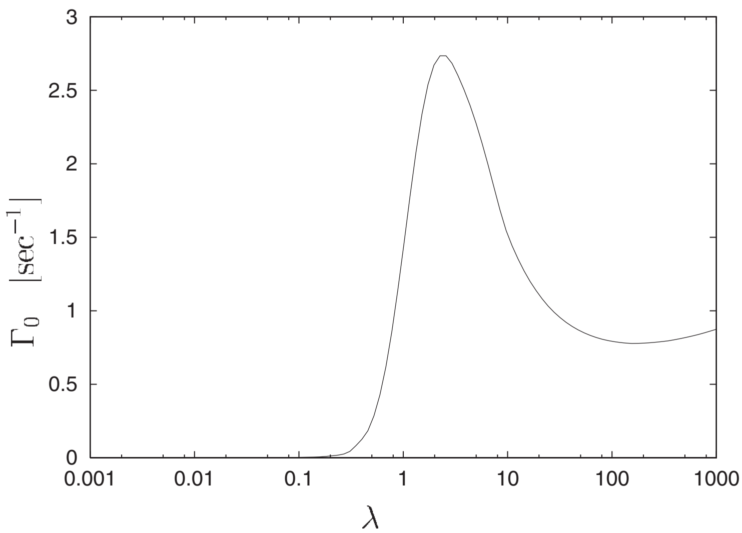

Figure 6. The decay rate Γ_0 as a function of the asymmetry parameter λ for $\nu = 953$ s^{-1}, $a_0/a = -2.13 \times 10^3$ and $\delta = 5.0 \times 10^{-3}$.

with

$$a(m) = 2(m^4 - m^2 + 1) \tag{70}$$

$$b(m) = (1 - m^2)(m^2 - 2). \tag{71}$$

For $E \to 0$, we have $(1 - m^2)\sinh(\omega_0\beta h/2) \to 8$, $a(m)E(m) + b(m)K(m) \to 2$ and $q_0, q_1 \to 0$, $q_2 \to 1$, so that $A(\beta) \to 4\sqrt{\omega_0^3/\pi h}$, which reproduces the zero-temperature decay rate Γ_0. Let us turn now to the limit $E \to 1$, where the period behaves as

$$\beta h = \frac{2\pi}{\omega_0}\left(1 + \frac{5}{36}(1 - E) + \cdots\right). \tag{72}$$

The leading term gives a crossover temperature $\beta_c^{-1} = h\omega_0/2\pi$ [19], i.e. for $\beta^{-1} > \beta_c^{-1}$ the decay rate is given by the familiar Arrhenuis–Kramers formula [20]. On the other hand, for $\beta^{-1} < \beta_c^{-1}$ the macroscopic tunnelling through the barrier becomes more probable, and the decay rate is given by (68). Recalling the energy unit U_0 defined by (55) and (58) we find

$$\beta_c^{-1} = \frac{h\omega_0}{2\pi}\left(\frac{U_0}{k_B}\right) = \frac{\hbar\nu\alpha}{2\pi k_B}\delta^{1/4}(1 + \mathcal{O}(\delta^{1/2})). \tag{73}$$

For small $(\beta - \beta_c)/\beta_c > 0$, from (65) and (69), we obtain the bounce action

$$\frac{S_{cl}}{h} \simeq \beta - \frac{18}{5}\beta_c\left(\frac{\beta - \beta_c}{\beta_c}\right)^2 \tag{74}$$

and

$$A(\beta) \simeq \sqrt{\frac{8\omega_0^3}{15h\pi^2}}\sinh\left(\frac{\omega_0\beta h}{2}\right)\left(1 - \frac{77}{20}\left(\frac{\beta - \beta_c}{\beta_c}\right) + \frac{20\,867}{2400}\left(\frac{\beta - \beta_c}{\beta_c}\right)^2\right). \tag{75}$$

4. Conclusion

In this paper we have investigated the macroscopic tunnelling of the metastable condensate of ^{7}Li. When the number of particles in the condensate exceeds a critical value $N^* = \sqrt{\pi/2}P^* a_0/a$, the metastable condensate no longer exists and the equation giving critical points has no solutions. In a region extremely close to N^*, i.e. $\delta = 1 - P/P^* \ll 1$, we have shown that the action takes a rather simple form (57), and explicitly calculated the decay rate of the metastable condensate using the WKB approximation.

Finally we make some remarks on our results. In order to justify the WKB approximation, we should choose the effective Planck's constant h to satisfy the condition $h \ll 1$. On the other hand, for very small h, it is impossible to observe the macroscopic tunnelling; the formula (60) provides an estimate of the tunnelling decay rate, $\Gamma_0 \sim \mathcal{O}(\mathrm{e}^{-1/h})$. This implies rather severe conditions on the parameter δ through the equation (58). If we use the experimental data at Rice University for the trapping potential [14, 15]; $\lambda \simeq 0.867$, $a_0/a \simeq -2.13 \times 10^3$ and $\nu \simeq 953\ \mathrm{s}^{-1}$, then the conditions are given by $h \simeq 2.92 \times 10^{-4}\ \delta^{-5/4} \ll 1$ and $\Gamma_0 \simeq 8.17 \times 10^5\ \delta^{7/8} \exp(-6.72 \times 10^3\ \delta^{5/4}) \sim \mathcal{O}(1)\ \mathrm{s}^{-1}$. Consequently, we have a typical region $3.0 \times 10^{-3} < \delta < 7.0 \times 10^{-3}$. Temperature effects on the tunnelling decay rate are estimated by using the equations (74) and (75): $\Gamma(\beta)$ is monotonically decreasing for $\beta > \beta_c$ and hence $\Delta\Gamma = \Gamma(\beta) - \Gamma_0 < \Gamma(\beta_c) - \Gamma_0$. For instance, for $\delta = 5.0 \times 10^{-3}$ the decay rate at zero temperature is $\Gamma_0 \simeq 1.03\ \mathrm{s}^{-1}$ and $\Delta\Gamma < 2.79\ \mathrm{s}^{-1}$. The crossover temperature is then given by $\beta_c^{-1} \simeq 1.02$ nK, which may be a realizable temperature in the experiments. The details of a crossover region have been discussed in [19]; there is a narrow crossover region of $\mathcal{O}(h^{3/2})$, where the decay rate is given by

$$\Gamma(\beta)T_0 \simeq \sqrt{\frac{8\omega_0^3}{15h\pi^2}} \sinh\left(\frac{\omega_0\beta h}{2}\right) \mathrm{erf}\left[\sqrt{\frac{36}{5\beta_c}}(\beta - \beta_c)\right] \exp\left[-\beta + \frac{18\beta_c}{5}\left(\frac{\beta - \beta_c}{\beta_c}\right)^2\right] \tag{76}$$

with $\mathrm{erf}(x) = (2\pi)^{-1/2} \int_{-\infty}^{x} \mathrm{d}y\ \exp(-y^2/2)$. For very small $h \ll 10^{-2}$, this formula matches smoothly onto (68) and $\Gamma(\beta)T_0 = (\omega_0/2\pi)[\sinh(\omega_0\beta h/2)/\sin(\omega_0\beta h/2)]\exp(-\beta)$ (Arrhenuis–Kramers formula) near β_c. However, we cannot apply the formula to the macroscopic tunnelling since the value of h in our situation is too large. We leave the issue of the crossover region for future research. The shape of the trapping potential also has some effect on the behaviour of the decay rate Γ_0: as shown in figure 6, the effect is significant for the disc-shaped potential ($\lambda > 1$), although it is rather small for the cigar-shaped potential ($\lambda \ll 1$) and Γ_0 is of the order of $10^{-3}\ \mathrm{s}^{-1}$, independent of λ.

References

[1] Dalfovo F, Giorgini S, Pitaevskii L P and Stringari S 1999 *Rev. Mod. Phys.* **71** 463
[2] Gross E P 1961 *Nuovo Cimento* **20** 454
[3] Pitaevskii L P 1961 *Sov. Phys.–JETP* **13** 451
[4] Moerdijk A J, Stwalley W C, Hulet R G and Verhaar B J 1994 *Phys. Rev. Lett.* **72** 40
[5] Abraham E R I, McAlexander W I, Sackett C A and Hulet R G 1995 *Phys. Rev. Lett.* **74** 1315
[6] Pérez-García V M, Michinel H, Cirac J I, Lewenstein M and Zoller P 1996 *Phys. Rev. Lett.* **77** 5320
Pérez-García V M, Michinel H, Cirac J I, Lewenstein M and Zoller P 1997 *Phys. Rev.* A **56** 1424
[7] Stoof H T C 1997 *J. Stat. Phys.* **87** 1353
[8] Parola A, Salasnich L and Reatto L 1998 *Phys. Rev.* A **57** R3180
[9] Kerman A K and Koonin S E 1976 *Ann. Phys., NY* **100** 332
[10] Cooper F, Pi S and Stancioff P N 1986 *Phys. Rev.* D **34** 3831
[11] Ueda M and Leggett A J 1998 *Phys. Rev. Lett.* **80** 1576

[12] Huepe C, Métens S, Dewel G, Borckmans P and Brachet M E 1999 *Phys. Rev. Lett.* **82** 1616
[13] Kleinert H 1995 *Path Integrals in Quantum Mechanics Statistics and Polymer Physics* (Singapore: World Scientific)
[14] Bradley C C, Sackett C A and Hulet R G 1997 *Phys. Rev. Lett.* **78** 985
[15] Sackett C A, Bradley C C, Welling M and Hulet R G 1997 *Appl. Phys.* B **65** 433
[16] Zweger W 1983 *Z. Phys.* B **51** 301
[17] Gelfand I M and Yaglom A M 1960 *J. Math. Phys.* **1** 48
[18] Kleinert H and Chervyakov A 1998 *Phys. Lett.* A **245** 345
[19] Affleck I 1980 *Phys. Rev. Lett.* **46** 388
[20] Kramers H 1990 *Physica* **7** 284